

# Drying Kinetics and Quality Assessment of Noodles from *Piper sarmentosum* Roxb. (Kaduk) Leaves

Nur Ainani Zuyyin Jinin<sup>a</sup>, Mohammad Amil Zulhilmi Benjamin<sup>b</sup>, Mohd Azrie Awang<sup>a,c\*</sup>

<sup>a</sup>Faculty of Food Science and Nutrition, Universiti Malaysia Sabah, Jalan UMS, 88400 Kota Kinabalu, Sabah, Malaysia; <sup>b</sup>Borneo Research on Algesia, Inflammation and Neurodegeneration (BRAIN) Group, Faculty of Medicine and Health Sciences, Universiti Malaysia Sabah, Jalan UMS, 88400 Kota Kinabalu, Sabah, Malaysia; <sup>c</sup>Food Security Research Laboratory, Faculty of Food Science and Nutrition, Universiti Malaysia Sabah, 88400 Kota Kinabalu, Sabah, Malaysia

**Abstract** *Piper sarmentosum* Roxb., commonly known as 'Kaduk', is a plant that holds significant importance in various cultures for its culinary and medicinal properties in Southeast Asia. The drying behaviour of *P. sarmentosum* leaf-based noodles (PSLN) was represented by a thin-layer drying kinetic model. The PSLN underwent drying at various temperatures ranging from 40 to 80 °C, with an examination of six different drying kinetic models: Lewis, Page, Henderson-Pabis, two-term exponential, Logarithmic, and Midilli and Kucuk. Subsequently, the PSLN extract was analysed for total phenolic content (TPC) and total flavonoid content (TFC), as well as antioxidant activity using the 2,2-diphenyl-1-picrylhydrazyl (DPPH) assay. Evaluation of the appropriate drying kinetic model included the calculation of the coefficient of determination, as well as root mean square error, and chi-square values. Among the six models, the Midilli and Kucuk model emerged as the most accurate in describing the drying kinetics for PSLN, as indicated by its superior goodness of fit. The effective moisture diffusivity ranged from  $1.22 \times 10^{-8}$  to  $4.86 \times 10^{-8}$  m<sup>2</sup>/s, with an activation energy of 35.86 kJ/mol. PSLN dried at 50 °C exhibited higher TPC and TFC values of  $121.60 \pm 0.20$  mg GAE/g dry extract and  $2.05 \pm 0.00$  mg QE/g dry extract, respectively, compared to other temperatures. Furthermore, the DPPH activity in the PSLN exhibited an inhibition value of  $92.49 \pm 0.03\%$ . Overall, drying PSLN products at 50 °C is recommended for retaining phenolics, flavonoids, and antioxidant activity.

**Keywords:** *Piper sarmentosum*, noodle, drying kinetic, phenolics, flavonoids, antioxidant.

## Introduction

The popularity of noodle products has surged due to their versatility in cooking methods such as frying, boiling, and stir-frying. Originating in China, noodles have evolved into a staple food, with a rich history dating back to the Han Dynasty era, where they were considered a type of cake [1]. Over time, various types, sizes, thicknesses, and flavours of noodles have been developed to cater to diverse preferences. To meet the demands of producers and consumers, noodle production techniques have undergone improvements, focusing on technological advancements and nutritional enhancement through refining processes, ingredients, and methodologies [2]. Typically, wheat flour is mixed with water before it undergoes the kneading process. The dough is managed and kneaded in such a way that its structure, texture, and composition produce high-quality outcomes.

*Piper sarmentosum* Roxb., commonly called 'Kaduk' and belonging to the Piperaceae family, is renowned for its high antioxidant content, which is beneficial for hypertension, inflammation, diabetes, and bacterial infections. Consequently, it has been widely used in Malay traditional medicine in

\*For correspondence:

ma.awang@ums.edu.my

Received: 06 April 2024

Accepted: 23 July 2024

© Copyright Jinin. This article is distributed under the terms of the [Creative Commons Attribution License](#), which permits unrestricted use and redistribution provided that the original author and source are credited.

Southeast Asian countries due to its well-studied pharmacological properties, including anti-inflammatory, antituberculosis, antiplasmodial, anticarcinogenic, and hypoglycaemic activities [3]. Its rich antioxidant content is attributed to high levels of polyphenols and flavonoids [4]. Furthermore, *P. sarmentosum* contains various antioxidants such as alkaloids, amides, pyrones, sterols, and neolignane [5], in addition to vitamins C, E, and carotenoids [6]. While there are no specific scientific studies on the use of *P. sarmentosum* in noodles, other *Piper* species, such as *P. nigrum* (Sirih Melayu), are widely incorporated for their enhanced flavour and retention of bioactive compounds, making them valuable ingredients in food products [7,8].

The drying process serves as an effective means to prevent the growth of microorganisms and enzymatic reactions responsible for product spoilage, thereby extending product shelf-life [9]. It offers a cost-efficient preservation approach without the need for additional preservatives. The main objective is to eliminate moisture, which makes products vulnerable to spoilage by bacteria and degradation due to chemical processes [10]. However, during drying at high temperatures, there can be changes in composition, nutritive value, and physical properties that impact bioactive compounds such as phenolics and antioxidant activity [11]. According to Bonazzi *et al.* [12] and Vega-Gálvez *et al.* [13], high temperatures aid fast drying but may compromise product quality, while low temperatures maintain quality but reduce the drying rate. Drying methods can be natural or technology-based. Natural sunlight is cost-effective but weather-dependent, posing risks of product damage. Technology-based approaches involving machinery offer advantages like weather independence, space efficiency, and controlled drying conditions [14]. Among these, cabinet drying stands out as a commonly employed and cost-effective technological method. It is widely used for drying small to medium quantities of products across various industries. Cabinet dryers are relatively inexpensive to purchase and operate compared to more specialised drying systems like tunnel dryers and freeze dryers, which are typically larger in scale and involve higher initial investments and operating costs [15]. Thus, cabinet dryers are suitable for a wide range of applications, including drying and heating raw materials.

The utilisation of herbal product blends in food has garnered increasing demand among consumers, with *P. sarmentosum* standing out for its notable antioxidant properties and associated health benefits. Despite its recognition, the drying process of noodle products incorporating *P. sarmentosum* leaves remains underexplored and has received limited attention. This study addresses this gap by employing a thin-layer drying kinetic model to comprehensively understand the characteristics of these noodle products. The main aims of this study are twofold: firstly, to determine the best thin-layer drying kinetic model for *P. sarmentosum* leaf-based noodles (PSLN) at various temperatures (40 to 80 °C); and secondly, to evaluate the quality of these products during different drying conditions by assessing total phenolic content (TPC), total flavonoid content (TFC), and antioxidant activity.

## Materials and Methods

### Chemicals and Reagents

Methanol was sourced from Chemiz (Selangor, Malaysia), whereas 2,2-diphenyl-1-picrylhydrazyl (DPPH) reagent, aluminium chloride (AlCl<sub>3</sub>), Folin-Ciocalteu reagent, sodium carbonate (Na<sub>2</sub>CO<sub>3</sub>), quercetin, gallic acid, and ascorbic acid were provided by Merck (Darmstadt, Germany).

### Sample Preparation

*Piper sarmentosum* leaves were sourced from Kota Kinabalu, Sabah, Malaysia, and served as the raw materials for this study. The mature leaves underwent thorough washing with running tap water to eliminate any dirt, sand, and other debris from the leaf surface. They were then cut into lengths of approximately 35.0 ± 0.5 mm or about 3 cm, using a knife, followed by further cutting and finely chopping for convenience in subsequent steps. The finely chopped leaves were then spread and levelled on a tray for the drying process. Drying was conducted in a drying cabinet at 50 °C for 3 h, as per Pratama *et al.* [16] with slight modifications. After drying, *P. sarmentosum* leaves were ground into powder using a food grinder machine (EBM 9182, Elba, Borso Del Grappa, Italy). The powdered leaves were stored in an airtight container until further use.

### Noodle Formulation

All ingredients were meticulously weighed according to the specified formulation: 50.0% wheat flour, 12.0% rice flour, 32.4% water, 1.6% salt, and 4.0% *P. sarmentosum* leaf powder, ensuring a uniform mixture. After thorough mixing, the kneaded dough was allowed to rest at room temperature for 10 min to relax before rolling. This resting period facilitates easier rolling by ensuring even moisture distribution [17]. Subsequently, the dough was pressed and laminated to form continuous sheets, which were then

rolled through a sheeter to achieve the desired thickness. The dough sheets were continuously fed through the sheeter until reaching the desired thickness to form noodle sheets.

### Drying Procedure

A circular arrangement of noodle sheets was laid out on the drying tray following procedures outlined by Stephenus *et al.* [18]. The drying cabinet (CD-9, Shini, New Taipei, Taiwan) was adjusted to five temperatures: 40 °C, 50 °C, 60 °C, 70 °C, and 80 °C, as per the preheating instructions before the drying process. Prepared samples were positioned on the tray using aluminium baskets as a base. During drying, samples were periodically removed, weighed, and then returned to the drying cabinet. The weight reduction of samples was documented at 10-minute intervals for the first hour, 20-minute intervals for the subsequent hour, and 30-minute intervals thereafter, until three consecutive measurements indicated consistent weight.

### Estimation of Free Moisture Fraction

Eq. (1) was employed to calculate the free moisture fraction using the weight data:

$$\Psi = \frac{MC_{pt} - MC_{pe}}{MC_{p0} - MC_{pe}} \tag{1}$$

where  $\Psi$  represents the dimensionless free moisture fraction,  $MC_{pe}$  represents the equilibrium moisture content (g),  $MC_{pt}$  represents the moisture content (g) at time  $t$ , and  $MC_{p0}$  represents the initial moisture content (g).

The moisture ratio curve was generated by plotting the dimensionless free moisture fraction,  $\Psi$ , against time (min).

### Modelling of Thin-Layer Drying Kinetics

In this investigation, six kinetic models were utilised to determine the most appropriate model for illustrating the drying characteristics of PSLN. These models were applied to match experimental data with predicted data. The thin-layer drying kinetic models were employed in this study included Lewis [19], Page [20], Henderson and Pabis [21], two-term exponential [22,23], Logarithmic [24,25], and Midilli and Kucuk [23,26], as represented in Eq. (2) through Eq. (7), respectively:

$$\Psi = \exp(-kt) \tag{2}$$

$$\Psi = \exp(-kt^n) \tag{3}$$

$$\Psi = a \exp(-kt) \tag{4}$$

$$\Psi = a \exp(-kt) + (1 - a) \exp(-kat) \tag{5}$$

$$\Psi = a \exp(-kt) + b \tag{6}$$

$$\Psi = a \exp(-kt^n) + bt \tag{7}$$

where  $k$  and  $t$  represent the drying constant ( $\text{min}^{-1}$ ) and the drying time (min), respectively, while  $a$ ,  $b$ , and  $n$  represent the empirical constant.

The adequacy of the chosen models was compared and evaluated using statistical tools to find the most suitable method for modelling the drying kinetics of PSLN. Statistical metrics such as the coefficient of determination ( $R^2$ ), root mean square error (RMSE), and chi-square ( $\chi^2$ ) were employed. The respective statistical formulas for these parameters are detailed in Eq. (8) through Eq. (10), respectively:

$$R^2 = 1 - \frac{\sum_{i=1}^n (y_i - \hat{y}_i)^2}{\sum_{i=1}^n (y_i - \bar{y})^2} \tag{8}$$

$$RMSE = \sqrt{\frac{\sum_{i=1}^n (y_i - \hat{y}_i)^2}{n}} \tag{9}$$

$$\chi^2 = \sum_{i=1}^n \frac{(y_i - \hat{y}_i)^2}{\hat{y}_i} \tag{10}$$

where  $n$  represents the number of observations,  $y_i$  represents the observed values,  $\hat{y}_i$  represents the predicted values, and  $\bar{y}$  represents the mean of the actual values.

## Estimation of Drying Rate

Using Eq. (11), the drying rate was determined and then compared with experimental results:

$$DR = -\frac{d\Psi}{dt} \quad (11)$$

where DR represents the drying rate in 1/s, and t represents the drying time (s).

## Estimation of Effective Moisture Diffusivity

Eq. (12) represents the effective moisture diffusivity ( $D_{\text{eff}}$ ), which was calculated utilising Fick's second law [27]:

$$\Psi = \frac{8}{\pi^2} \sum_{n=1}^{\infty} \frac{1}{(2n+1)^2} \exp\left[-(2n+1)^2 \pi^2 \frac{D_{\text{eff}}}{4L^2} t\right] \quad (12)$$

where n represents the integer value,  $D_{\text{eff}}$  represents the effective moisture diffusivity ( $\text{m}^2/\text{s}$ ), L represents the thickness of the initial sample at half (m), and t represents the drying time (s).

For long drying times ( $\Psi < 0.6$ ), a limiting case was assumed and expressed logarithmically, as shown in Eq. (13):

$$\ln(\Psi) = \ln\left(\frac{8}{\pi^2}\right) - \left(\pi^2 \frac{D_{\text{eff}}}{4L^2} t\right) \quad (13)$$

where empirical data could be used to describe  $D_{\text{eff}}$  using the graph of  $\ln(\Psi)$  versus drying time (s).

When  $\ln(\Psi)$  is plotted against drying time (s), a straight line is obtained, with the sloped given by Eq. (14):

$$\text{Slope} = \pi^2 \frac{D_{\text{eff}}}{4L^2} \quad (14)$$

## Estimation of Activation Energy

Assuming the Arrhenius function governs the relationship between the  $D_{\text{eff}}$  and ambient temperature [27], Eq. (15) is formulated as follows:

$$D_{\text{eff}} = D_0 \exp\left(-\frac{E_a}{RT}\right) \quad (15)$$

Where  $D_0$  represents the preexponential factor ( $\text{m}^2/\text{s}$ ),  $E_a$  represents the activation energy (kJ/mol), R represents the universal gas constant ( $R = 8.314 \text{ J/mol}$ ), and T represents the absolute temperature (K).

Using exponential regression, the value of  $E_a$  (kJ/mol) can be calculated by plotting  $D_{\text{eff}}$  against  $1/RT$ .

## Sample Extraction

Sample extraction of PSLN was conducted following the protocols outlined by Assefa *et al.* [28] with minor adjustments. Approximately 2 g of PSLN was ground and combined with 40 mL of methanol solution. The extraction was performed using a water bath set at 60 °C for 30 min, with agitation at 100 rpm. After extraction, the sample was filtered through Whatman No. 1 filter paper (Maidstone, Kent, UK), and the resulting extract was refrigerated for subsequent analysis.

## Estimation of TPC and TFC

The TPC and TFC were determined using the Folin-Ciocalteu assay outlined by Stephenus *et al.* [18] and the aluminium colorimetric assay outlined by Jinoni *et al.* [29], respectively, with minor adaptations. For TPC determination, 500  $\mu\text{L}$  of the extract was mixed with 1.5 mL of  $\text{Na}_2\text{CO}_3$  solution and 500  $\mu\text{L}$  of Folin-Ciocalteu reagent. The mixture was diluted to 10 mL with distilled water, thoroughly shaken, and then incubated in darkness for 2 h. Absorbance was measured at 765 nm using a UV-Vis spectrophotometer (Lambda 25, Perkin Elmer, Waltham, MA, USA). For TFC determination, 2 mL of extract was mixed with 2 mL of 2%  $\text{AlCl}_3$  solution, incubated at room temperature in the dark for 15 min, and absorbance was measured at 430 nm. Using gallic acid and quercetin solutions as standards, linear

equations from calibration curves were used to quantify TPC and TFC as mg of gallic acid equivalents (GAE) and quercetin equivalents (QE) per gram of dry extract, respectively.

### Estimation of DPPH

To assess its antioxidant activity, the method proposed by Awang *et al.* [30] was used with slight modifications to determine the scavenging effect of DPPH radicals. Briefly, 2 mL of extract was mixed with 2 mL of DPPH solution prepared in methanol and kept in the dark for 30 min at ambient temperature. The absorbance of the resulting solution was then measured at 517 nm. Ascorbic acid served as a positive control in the comparative analysis. Eq. (16) was used to determine the activity of the extract towards scavenging DPPH radicals:

$$\text{DPPH free radical scavenging activity (\%)} = \frac{A_{\text{control}} - A_{\text{sample}}}{A_{\text{control}}} \times 100 \quad (16)$$

where  $A_{\text{sample}}$  represents the absorbance of the extract mixed with the DPPH solution, while  $A_{\text{control}}$  represents the absorbance of the DPPH solution without the extract.

### Statistical Analysis

The results from each experiment are presented as mean  $\pm$  standard deviation (SD), with three replicates conducted to ensure accuracy. Excel Solver (Microsoft Office 2019) was employed to calculate statistical metrics, such as  $R^2$ , RMSE, and  $\chi^2$ , which were essential for evaluating the goodness of fit of thin-layer drying kinetic models. Subsequently, the data were analysed using SPSS statistical software (Version 29). To assess the significance of different drying temperatures, comparisons were made at a 95% confidence level using one-way analysis of variance (ANOVA) with Tukey's Honestly Significant Difference (HSD) post hoc test. Additionally, a correlation analysis was conducted using the Pearson correlation coefficient ( $r$ ). Statistical significance was determined as  $p < 0.05$ , with  $p < 0.01$  considered extremely significant.

## Results and Discussion

### Effects of Drying Temperatures on Free Moisture Fraction

The behaviour of PSLN during the drying process is illustrated in Figure 1, which shows the variation in free moisture content over time at temperatures ranging from 40 to 80 °C. Although the drying curves at different temperatures exhibit similar trends, their drying rates vary. The time required to reach equilibrium moisture content differed as follows: 640 min at 40 °C, 540 min at 50 °C, 410 min at 60 °C, 340 min at 70 °C, and 180 min at 80 °C. Higher temperatures corresponded to faster drying rates and shorter durations to achieve equilibrium moisture content. Drying at 40 °C required a longer period to attain equilibrium moisture content, whereas drying at 80 °C resulted in quicker drying times compared to other temperatures. This observation aligns with the principle that heat transfer rates increase with higher drying temperatures, leading to accelerated mass and heat transfer processes [31]. This increased heat transfer promotes cell expansion and collapse, facilitating the formation of pores or micro-cavities on the tissue surface [32]. As a result, rapid moisture diffusion from the sample core to its surface is facilitated, reducing the overall drying time.

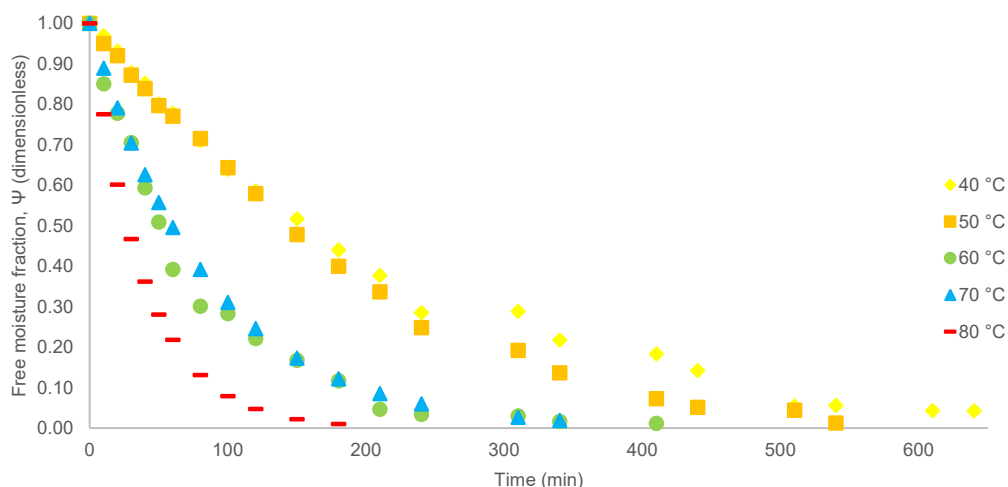


Figure 1. Ψ versus drying time of PSLN at various temperatures

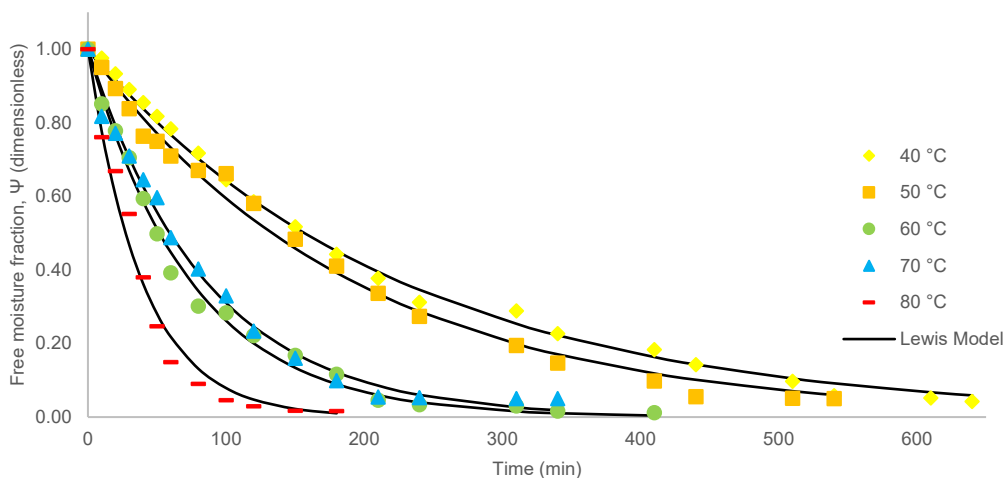
### Effects of Drying Temperatures on Drying Kinetic Models

Thin-layer drying kinetic models were employed in this study to estimate drying times and generate drying curves for PSLN. These models provide a unified description of drying phenomena, assuming uniform drying within the material and constant environmental conditions (relative humidity and temperature). By correlating moisture content at various times with drying parameters, these models offer a generalised depiction of the drying process, enabling accurate prediction of drying behaviour and optimisation of drying conditions. In this investigation, six thin-layer drying kinetic models—Lewis, Page, Henderson and Pabis, Logarithmic, two-term exponential, and Midilli and Kucuk were applied to elucidate the drying kinetics of PSLN across different temperatures. The model with the highest  $R^2$  value and the lowest RMSE and  $\chi^2$  values was selected as the benchmark for assessing goodness of fit. Table 1 presents the results of fitting experimental data to these various models. Additionally, Figure 2 compares experimental and predicted  $\Psi$  values for all models at different drying times, including predictions from the Lewis (A), Page (B), Henderson and Pabis (C), two-term exponential (D), Logarithmic (E), and Midilli and Kucuk (F) models at various temperatures.

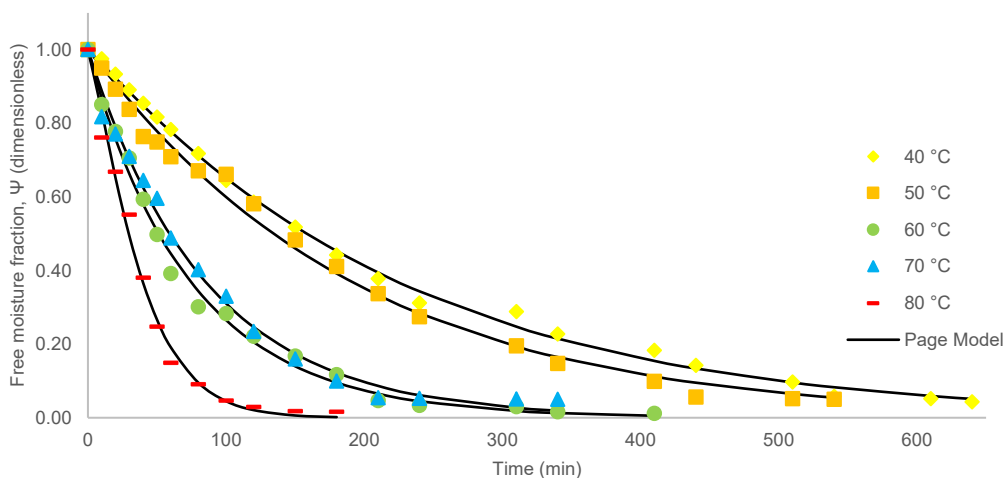
Table 1. Constant values and goodness of fit for thin-layer drying kinetic models of PSLN at various temperatures

Model	Temperature (°C)	Constant	$R^2$	RMSE ( $10^{-4}$ )	$\chi^2$ ( $10^{-4}$ )
Lewis	40	k = 0.004	0.997	1.620	0.166
	50	k = 0.005	0.993	3.948	0.744
	60	k = 0.013	0.994	3.239	0.338
	70	k = 0.012	0.993	3.824	0.306
	80	k = 0.025	0.983	9.617	0.789
Page	40	k = 0.004 n = 1.043	0.998	1.300	0.051
	50	k = 0.004 n = 1.030	0.993	3.803	1.070
	60	k = 0.015 n = 0.971	0.994	3.127	1.177
	70	k = 0.012 n = 0.995	0.993	3.821	0.026
	80	k = 0.011 n = 1.228	0.991	5.270	0.072

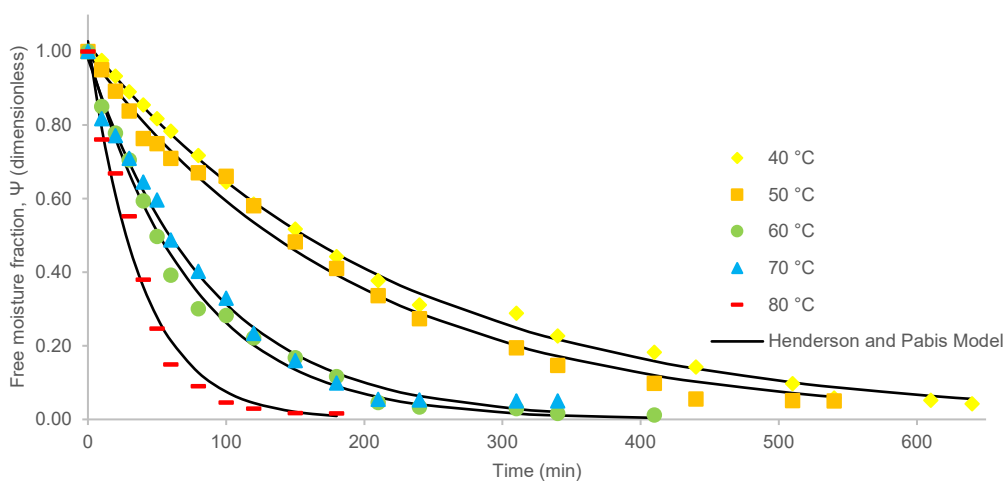
Model	Temperature (°C)	Constant	R <sup>2</sup>	RMSE (10 <sup>-4</sup> )	χ <sup>2</sup> (10 <sup>-4</sup> )
Henderson and Pabis	40	a = 1.018 k = 0.005	0.998	1.259	0.028
	50	a = 0.995 k = 0.005	0.993	3.918	0.479
	60	a = 0.995 k = 0.013	0.994	3.220	0.485
	70	a = 0.981 k = 0.011	0.993	3.531	0.005
	80	a = 1.027 k = 0.026	0.984	9.090	2.864
Two-term Exponential	40	a = 1.425 k = 0.005	0.998	1.397	0.124
	50	a = 0.007 k = 0.742	0.993	3.908	0.499
	60	a = 0.010 k = 1.297	0.994	3.203	0.396
	70	a = 0.029 k = 0.386	0.993	3.350	0.067
	80	a = 1.750 k = 0.035	0.991	5.138	0.270
Logarithmic	40	a = 1.029 k = 0.004 b = -0.014	0.998	1.198	0.000
	50	a = 1.050 k = 0.004 b = -0.070	0.995	2.786	0.000
	60	a = 0.987 k = 0.014 b = 0.012	0.994	3.060	0.000
	70	a = 0.982 k = 0.011 b = -0.002	0.993	3.528	0.000
	80	a = 1.049 k = 0.024 b = -0.028	0.986	8.234	0.000
Midilli and Kucuk	40	a = 1.016 k = 0.005 n = 0.995 b = 0.000	0.998	1.183	0.000
	50	a = 0.982 k = 0.005 n = 1.001 b = 0.000	0.995	2.863	0.001
	60	a = 1.003 k = 0.015 n = 0.979 b = 0.000	0.994	3.070	0.003
	70	a = 0.957 k = 0.007 n = 1.110 b = 0.000	0.994	3.068	0.013
	80	a = 0.970 k = 0.008 n = 1.320 b = 0.000	0.992	4.763	0.009



**A**



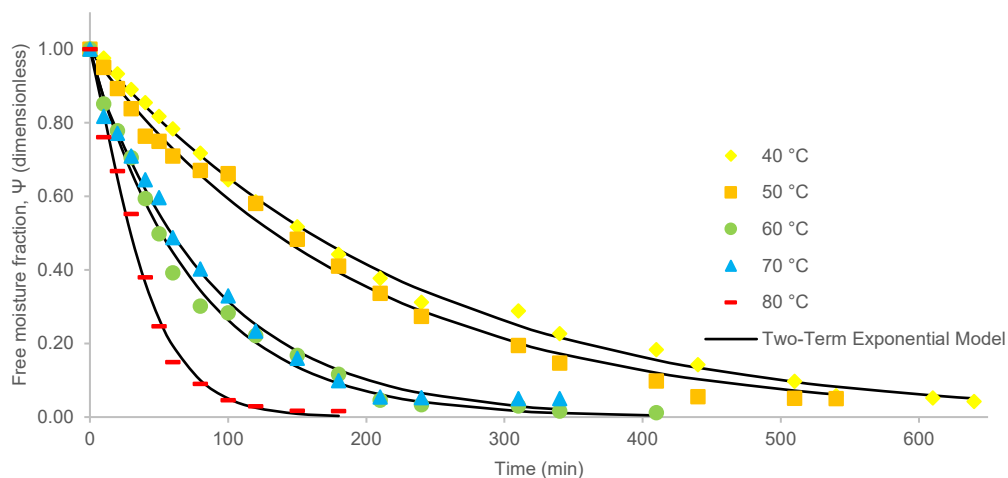
**B**



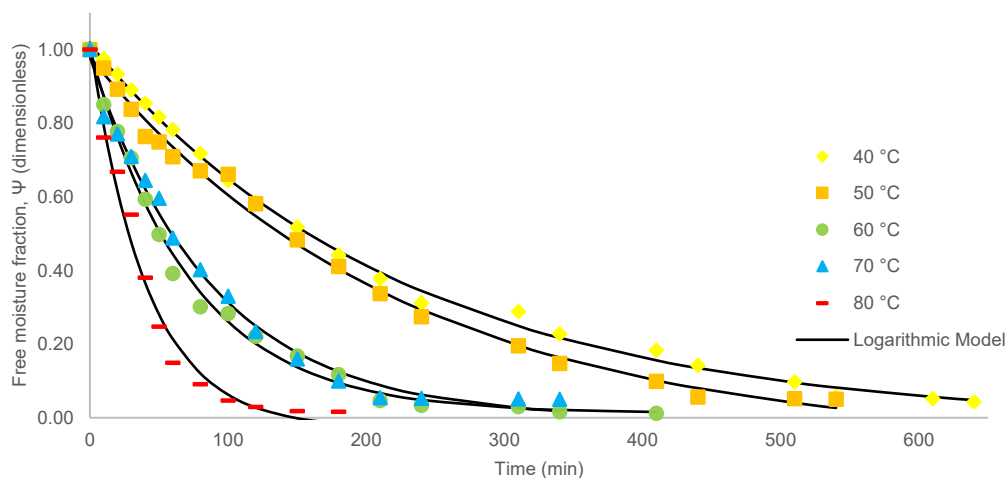
**C**

*Continue to next page*

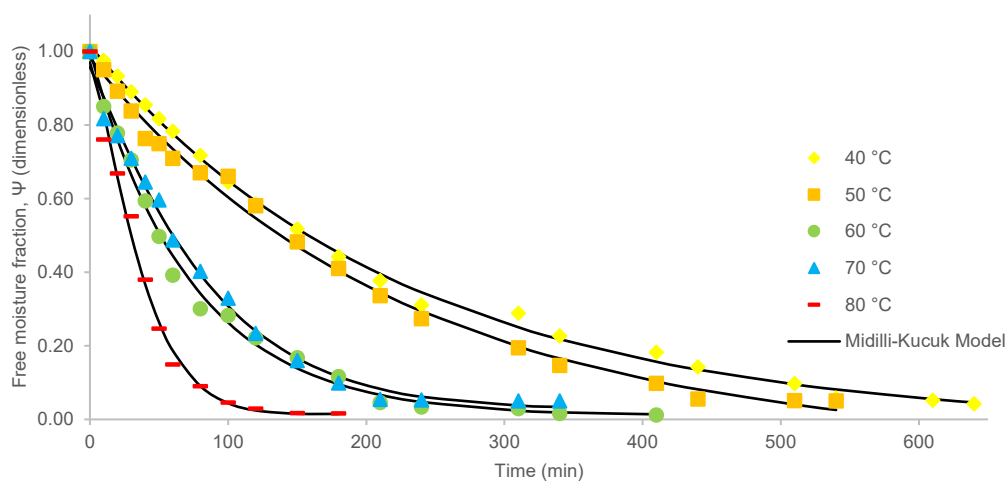




D



E



F

**Figure 2.** Drying curves of PSLN at various temperatures showing experimental and predicted data based on mathematical modelling

The following variations were observed in the  $R^2$  values: the Lewis model exhibited a range from 0.983 to 0.997, the Page model from 0.991 to 0.998, the Henderson and Pabis model from 0.984 to 0.998, the two-term exponential model from 0.991 to 0.998, the Logarithmic model from 0.986 to 0.998, and the Midilli and Kucuk model from 0.992 to 0.998. A satisfactory fit is indicated when the  $R^2$  values for the models surpass the acceptable threshold of 0.900 [33]. Therefore, the  $R^2$  values close to 1.000 for all drying temperatures indicate a strong correlation between the models and the data. Furthermore, the range of RMSE values for the five temperatures was as follows: the Lewis model ranges from  $1.620 \times 10^{-4}$  to  $9.617 \times 10^{-4}$ , the Page model from  $1.300 \times 10^{-4}$  to  $5.270 \times 10^{-4}$ , the Henderson and Pabis model from  $1.259 \times 10^{-4}$  to  $9.090 \times 10^{-4}$ , the two-term exponential model from  $1.397 \times 10^{-4}$  to  $5.138 \times 10^{-4}$ , the Logarithmic model from  $1.198 \times 10^{-4}$  to  $8.234 \times 10^{-4}$ , and the Midilli and Kucuk model from  $1.183 \times 10^{-4}$  to  $4.763 \times 10^{-4}$ . Another pivotal metric used to ascertain the soundness of the models is the  $\chi^2$  value. The minimum  $\chi^2$  values were documented as follows: the Lewis model ranges from  $0.166 \times 10^{-4}$  to  $0.789 \times 10^{-4}$ , the Page model from  $0.026 \times 10^{-4}$  to  $1.177 \times 10^{-4}$ , the Henderson and Pabis model from  $0.005 \times 10^{-4}$  to  $2.864 \times 10^{-4}$ , the two-term exponential model from  $0.067 \times 10^{-4}$  to  $0.499 \times 10^{-4}$ , the Logarithmic model was  $0.000 \times 10^{-4}$ , and the Midilli and Kucuk model from  $0.000 \times 10^{-4}$  to  $0.013 \times 10^{-4}$ . Moreover, a notable observation was that the constant values exhibited by each model under identical dehydration conditions were comparatively consistent.

Overall, the  $R^2$  value obtained at all temperatures for the Midilli and Kucuk model was  $> 0.992$ . Additionally, the RMSE and  $\chi^2$  values for this model were lower compared to the other models, albeit slightly higher than those for the Logarithmic model. From the  $R^2$ , RMSE, and  $\chi^2$  data, it is possible to conclude that the Midilli and Kucuk model adequately fitted the drying curve and precisely predicted PSLN drying behaviour. This conclusion is supported by several studies where the Midilli and Kucuk model exhibited excellent fitting ability in predicting drying behaviour for various food products such as green seaweed [33], sweet potato slices [34], and Chinese saffron [35]. Apart from constant  $b$ , which remained constant at 0.000, it was observed that the drying constant ( $k$ ) and empirical constants ( $a$  and  $n$ ) for PSLN, as predicted by the Midilli and Kucuk model, changed as the temperature rose. This indicates that the model's constants are not solely dependent on rising temperatures. To sum up, the Midilli and Kucuk model emerges as a promising approach for characterising the drying kinetics of diverse food products. Hence, due to their consistent goodness-of-fit parameters throughout the study, the Midilli and Kucuk model emerged as the most suitable method for depicting the drying kinetics of PSLN across temperatures ranging from 40 °C to 80 °C. Consequently, by utilising thin-layer drying kinetics modelling to analyse food products, critical information regarding air velocity, optimal drying duration, relative humidity, temperature, and storage conditions can be obtained [36]. Armed with this comprehensive data, it becomes feasible to design more efficient dryers and potentially streamline processes, thereby mitigating postharvest losses.

The Lewis model, a simplified form of the diffusion model, posits that the drying rate is proportional to the difference between the instantaneous moisture content of the material and its equilibrium value. Analogous to Newton's law of cooling, this model assumes that the resistance to moisture flow is concentrated in a surface layer of the drying material [36]. While widely used in drying studies, the Lewis model does not fully describe the entire drying curve. To address this limitation, the Page model and other two-term and multiple-term exponential models introduce empirical exponents or additional terms, providing a more accurate representation of drying kinetics. Based on the findings, Midilli and Kucuk stands out the effective in describing the drying behaviour of PSLN. The Midilli and Kucuk model is a two-parameter empirical model widely used to describe thin-layer drying kinetics. It incorporates both the drying rate constant and the moisture content dependency in its equation, making it suitable for various agricultural and food products [37]. The model assumes that the drying process occurs under constant drying conditions with uniform temperature and air velocity. Moisture transfer is primarily governed by Fick's second law of diffusion, where the driving force is the moisture gradient within the material. The versatility of the Midilli and Kucuk model lies in its ability to fit experimental drying data well across different temperature and relative humidity conditions, providing insights into the moisture removal kinetics during drying processes.

### Effects of Drying Temperatures on Drying Rate

Figure 3 depicts the drying rate curves of the process relative to moisture content, demonstrating a gradual increase in drying rate across all temperatures. This elevation in drying rate alongside the  $\Psi$  increment occurs because, as moisture content diminishes during drying, more energy becomes available to facilitate further moisture removal [38]. This phenomenon is commonly observed in drying processes, where the rate of moisture removal escalates as the drying process advances and moisture

content declines. In line with previous research on the convective drying of *P. macrocarpa* fruits [18], the moisture content measurements of PSLN at the conclusion of the drying process indicate successful removal of water from the product. In summary, the results indicate that drying rate increases as drying temperature rises and initial sample size decreases.

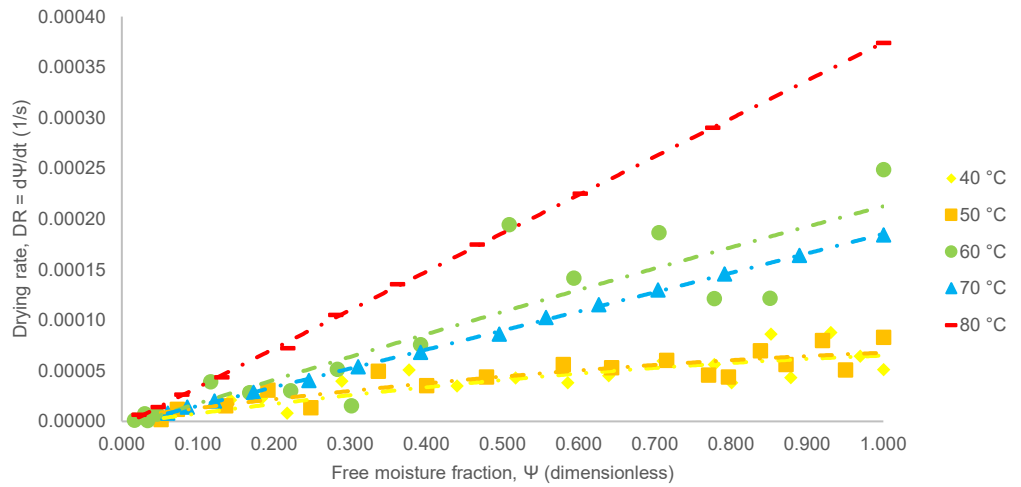


Figure 3. DR versus  $\Psi$  of PSLN at various temperatures

### Effects of Drying Temperatures on Effective Moisture Diffusivity

The diffusivity kinetic models utilised in this study interpret the drying process by optimising estimated values based on various model assumptions, including boundary conditions, geometry, and the physical and transport properties relevant to both isothermal and non-isothermal drying processes. The  $D_{eff}$  used in these models does not directly account for the driving force, which in this context is the moisture gradient. Assumptions inherent to these models include equilibrium between the surface moisture content of the product and the temperature and relative humidity of the surrounding air, as well as the stability of the diffusion coefficient throughout the drying process. The  $D_{eff}$  was determined by analysing the correlation between  $\ln(\Psi)$  and drying time (s) across a range of temperatures (Figure 4). The  $D_{eff}$  was calculated using the gradient of each linear regression plot.

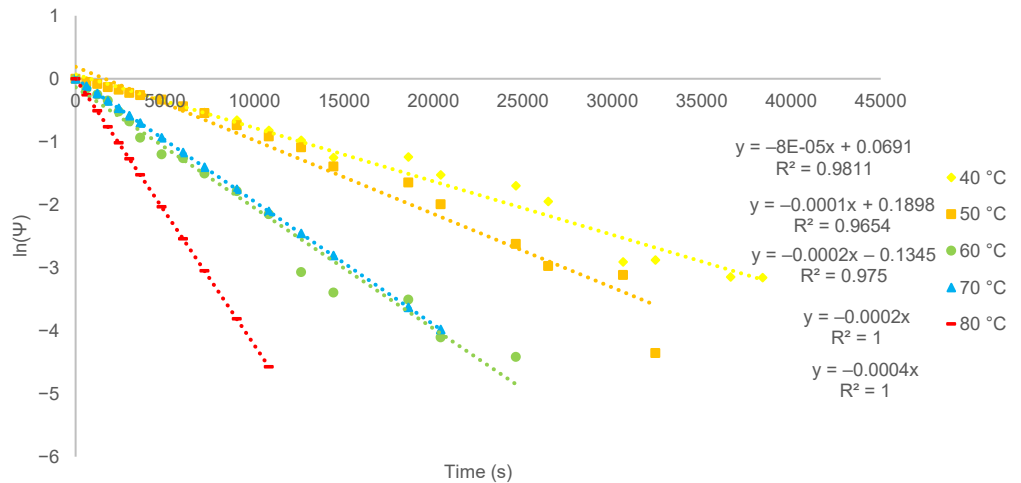


Figure 4.  $\ln(\Psi)$  versus drying time of PSLN at various temperatures

The data in Table 2 illustrates the variation in the  $D_{\text{eff}}$  at various temperatures, showing a significant increase from  $1.22 \times 10^{-8}$  to  $4.86 \times 10^{-8}$  m<sup>2</sup>/s. This finding is consistent with previous investigations that reported values ranging from  $10^{-6}$  to  $10^{-12}$  m<sup>2</sup>/s for conventional food dehydration processes [39]. Various drying methods have been studied to assess whether the  $D_{\text{eff}}$  of different products changes during drying. However, regardless of whether a hot air dryer or a thermal convection oven is used, the  $D_{\text{eff}}$  tends to increase with higher temperatures across different drying techniques [40]. This increase is attributed to greater heat absorption in the material at higher temperatures, thereby enhancing mass transfer rates [32]. Thus, the  $D_{\text{eff}}$  is significantly influenced by the rise in drying temperature.

**Table 2.**  $D_{\text{eff}}$  parameters of PSLN at various temperatures

Temperature (°C)	Slope ( $k_0$ )	$D_{\text{eff}} \times 10^{-8}$ (m <sup>2</sup> /s)	$R^2$
40	-0.00008	1.22	0.9811
50	-0.0001	1.62	0.9654
60	-0.0002	2.84	0.9750
70	-0.0002	3.24	1.0000
80	-0.0004	4.86	1.0000

### Effects of Drying Temperatures on Activation Energy

The  $E_a$  represents the minimum energy required to initiate the moisture extraction process from a specific substance. By applying the Arrhenius equation, an exponential regression graph was constructed to examine the relationship between  $D_{\text{eff}}$  against  $1/RT$ . This graph enabled the calculation of the  $E_a$  of PSLN in relation to drying temperature [36]. The exponential regression analysis shown in Figure 5 revealed that PSLN has an  $E_a$  of 35.86 kJ/mol, indicating that a significant amount of energy is needed to remove moisture from the substance during drying. In the scientific literature, the  $E_a$  required for dehydrating food products typically ranges from 14.42 to 43.26 kJ/mol [36]. The  $E_a$  obtained in this study aligns closely with findings reported for food products such as pumpkin (33.15 kJ/mol) and banana slices (32.65 kJ/mol) [41,42]. However, discrepancies may arise due to variations in drying methods, materials, and operational parameters used during the drying process.

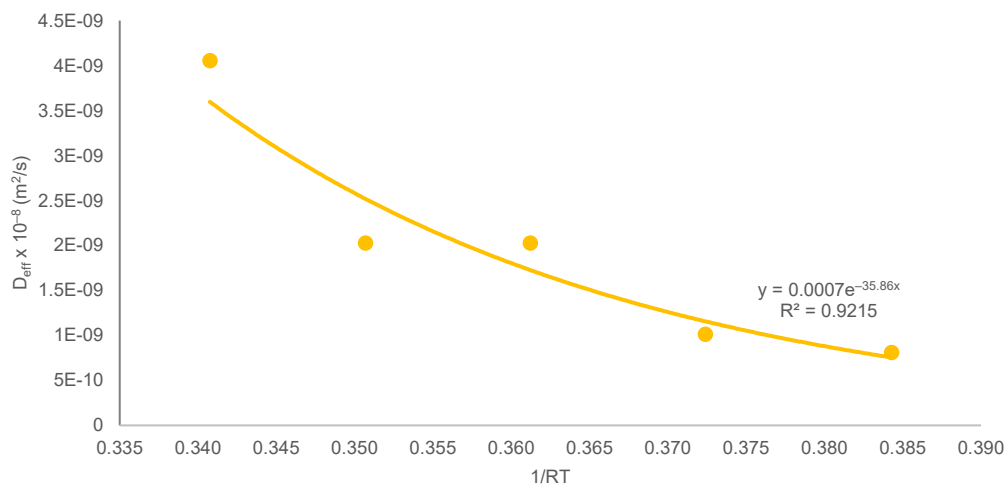


**Figure 5.**  $D_{\text{eff}}$  versus  $1/RT$  according to the Arrhenius model for PSLN

### Effects of Drying Temperatures on TPC and TFC

The TPC and TFC in PSLN extracts are depicted in Figure 6. Based on the TPC findings, it was observed that PSLN extracts conducted at 40 °C yielded the lowest TPC ( $87.13 \pm 0.06$  mg GAE/g dry extract) compared to other temperatures. Subsequent minimum TPC values were determined at 50 °C ( $121.60 \pm 0.20$  mg GAE/g dry extract), 60 °C ( $119.93 \pm 1.34$  mg GAE/g dry extract), 70 °C ( $118.43 \pm 0.06$  mg GAE/g dry extract), and 80 °C ( $110.10 \pm 0.00$  mg GAE/g dry extract). Rababah *et al.* [43] suggested that the decreased in TPC at 40 °C could be attributed to the drying process, particularly when herbal plants

like *P. sarmentosum* leaves are involved, which may lead to approximately a 30% reduction in polyphenol content. Additionally, Al-Hamdani *et al.* [44] indicated that studies on solar drying, involving moderate heat ( $\leq 50$  °C), could affect the concentration of phenolic sugar bonds and the formation of phenolics, potentially increasing TPC. Babu *et al.* [45] also support that drying temperatures between 50–60 °C minimise phenolic quality loss, making them suitable for product applications.

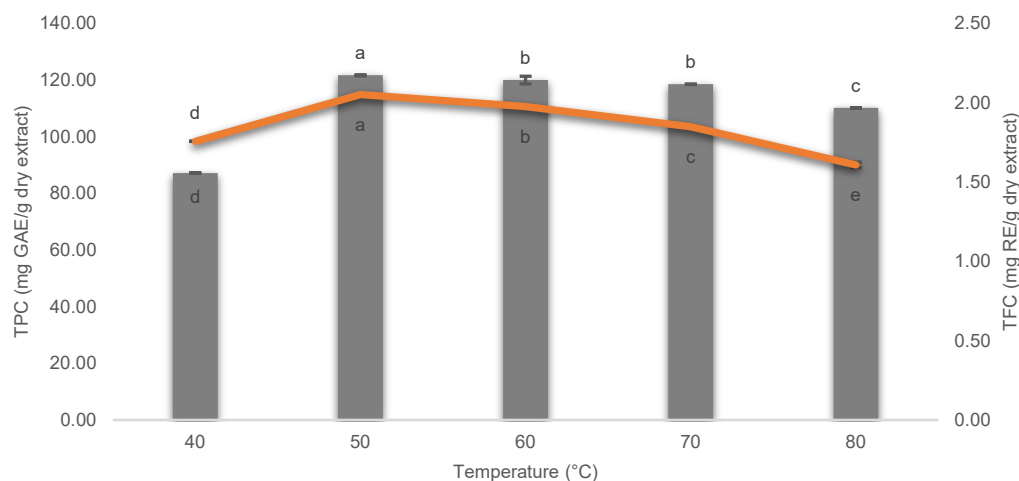


**Figure 6.** TPC (bar graph) and TFC (line graph) of PSLN extract at various temperatures. The data presents mean  $\pm$  SD from triplicates. The letters within the bars and lines represent the variables that have been determined to have statistically significant differences (ANOVA, Tukey's HSD test,  $p < 0.05$ )

The highest TFC value was observed at 50 °C, showing a more pronounced increase compared to other temperatures, i.e.,  $2.05 \pm 0.00$  mg QE/g dry extract. This result is consistent with the findings of a prior investigation conducted by Ifrada *et al.* [46], wherein TFC concentrations were greatest at 50 °C (0.46 mg QE/g). Additionally, a temperature of 50.24 °C was reported to be optimal for obtaining the highest TFC yield of *Pueraria lobata* [47]. In contrast, the PSLN extract exhibited the lowest TFC concentration of  $1.61 \pm 0.02$  mg QE/g dry extract when dried at 80 °C. The following TFC values were observed at other temperatures:  $1.76 \pm 0.00$  mg QE/g dry extract at 40 °C,  $1.98 \pm 0.00$  mg QE/g dry extract at 60 °C, and  $1.85 \pm 0.01$  mg QE/g dry extract at 70 °C. Based on this study, the PSLN extracts at 50 °C exhibited a significantly higher value compared to other temperatures. Higher temperatures may further decrease the TFC. As a result, the optimal dehydration temperature for PSLN extracts to preserve phenolics and flavonoids is 50 °C.

### Effects of Drying Temperatures on DPPH Radical Scavenging Activity

The DPPH assay revealed that the antioxidants present in the PSLN extract effectively converted DPPH radicals to DPPH-H molecules, resulting in a discernible colour change from purple to yellow and a reduction in absorbance at 517 nm [48]. Figure 7 illustrates the inhibition of DPPH radicals at various drying temperatures. The antioxidant activity, measured as DPPH radicals, at 40, 50, 60, 70, and 80 °C was  $89.91 \pm 0.52\%$ ,  $92.49 \pm 0.03\%$ ,  $91.06 \pm 0.07\%$ ,  $89.52 \pm 0.13\%$ , and  $87.72 \pm 0.04\%$ , respectively. Notably, the PSLN extract at 50 °C exhibited significantly higher antioxidant activity compared to other temperatures. Ngamsuk *et al.* [48] suggested that DPPH radical scavenging activity increased with a rise in drying temperature to 50 °C for processed *Coffea arabica* leaves. However, the assessment of herb antioxidant properties can be influenced by the ingredient preparation methods in food product manufacturing, such as noodles enriched with plants. These findings corroborate those of Sadek and Hamidah [49], who observed an increase in DPPH free radical scavenging activity in sorghum-moringa substituted tapioca noodles after the drying process, proposing them as alternative antioxidant sources. Additionally, Ahmad *et al.* [50] showed that the incorporation of fenugreek seed powder in noodles led to a significant increase in DPPH values, ranging from 31–42%, with the greatest enhancement in noodles. This highlights the potential to enhance DPPH radical scavenging capacity in noodles supplemented with herbal powders. Therefore, based on the results of the study, the optimal drying temperature for PSLN extract was determined to be 50 °C to achieve maximum antioxidant activity.

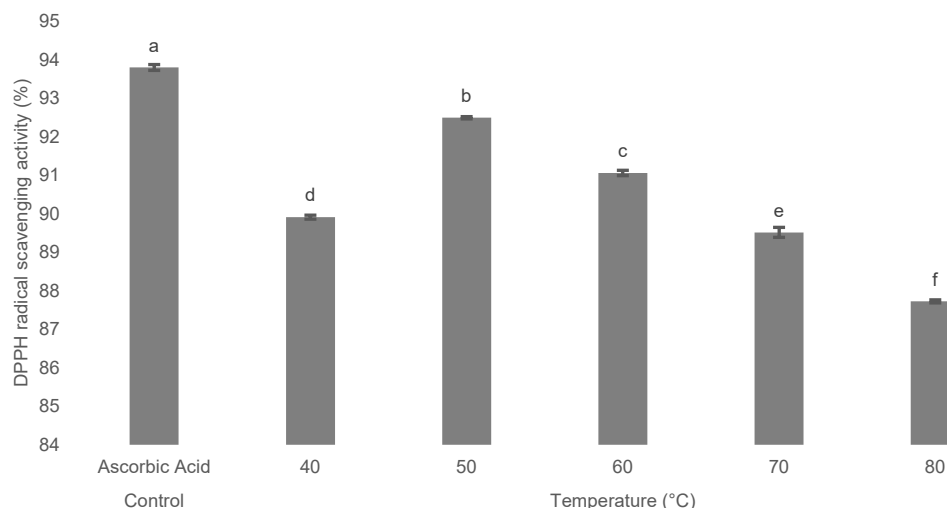


**Figure 7.** DPPH radical scavenging activity of PSLN extract at various temperatures. The data presents mean ± SD from triplicates. The letters within the bars represent the variables that have been determined to have statistically significant differences (ANOVA, Tukey's HSD test,  $p < 0.05$ ). Ascorbic acid served as the positive control

### Correlation Analysis

The antioxidant activity of plant materials is strongly correlated with the abundance of phenolics and flavonoids [51]. To ascertain this connection, the correlation between TPC/TFC and DPPH of the PSLN extract was examined (Table 3). Briefly, the results of the correlation coefficients for the PSLN extract indicated that there was a high positive correlation between TFC and DPPH ( $r = 0.957$ ), whereas there was a weak positive association between TPC and DPPH ( $r = 0.354$ ). The weaker correlation observed in TPC-DPPH might be attributed to the diverse structures and antioxidant properties of phenolics, as they constitute a diverse group of chemicals [52]. Nevertheless, higher TFC values contribute to increased antioxidant activity, as flavonoids possess the ability to donate hydrogen atoms to free radicals, thereby deactivating them [51]. Therefore, the results confirm that the presence of flavonoids is strongly associated with antioxidant activity.

**Table 3.** Correlation analysis between TPC/TFC and DPPH of PSLN extract

Antioxidant Activity	TPC		TFC	
	r	p-Value	r	p-Value
DPPH	0.354	0.005	0.957*	0.032

\*Correlation is significant at  $p < 0.01$  (2-tailed).

### Limitations and Future Research

While the study significantly contributes to the application of drying kinetics and quality assessment for PSLN, it is constrained by several limitations. These include assumptions that temperature and the surface moisture content of the product are in equilibrium with the surroundings, leading to Eq. (15) inadequately describing the drying data across the entire range. Furthermore, the use of methanol for extraction may not fully reflect real-world scenarios. Future research could explore more realistic boundary conditions in solving the diffusion equation, as well as the use of food-safe solvents. Addressing these challenges will refine the understanding of drying kinetics and enhance the applicability of findings in the food industry. Additionally, the incorporation of *P. sarmentosum* leaves into noodles is a novel innovation, particularly in terms of sensory attributes. Rigorous evaluations and consumer studies are essential to refine formulation and enhance the market potential of PSLN, ensuring its taste profile aligns with broad consumer acceptance.

## Conclusions

Overall, this study highlights the significance of selecting optimal drying parameters for PSLN. The relationship between higher drying temperatures and reduced drying times supports the suitability of the Midilli and Kucuk model for thin-layer drying kinetics, demonstrating superior goodness of fit with  $R^2$  values exceeding 0.920, and minimal RMSE ( $< 4.763 \times 10^{-4}$ ) and  $\chi^2$  ( $< 0.013 \times 10^{-4}$ ). The  $D_{\text{eff}}$  ranged from  $1.22 \times 10^{-8}$  to  $4.86 \times 10^{-8}$  m<sup>2</sup>/s, with an  $E_a$  of 35.86 kJ/mol. The highest TPC ( $121.60 \pm 0.20$  mg GAE/g dry extract) and TFC ( $2.05 \pm 0.00$  mg QE/g dry extract) values were achieved at 50 °C. Antioxidant activity was also notably high at 50 °C ( $92.49\% \pm 0.02$ ). This comprehensive understanding of drying kinetics and its impact on phenolics, flavonoids, and antioxidant activity provides valuable insights for optimising the production process and improving the nutritional and functional qualities of PSLN. These findings can be applied to develop new food products with health benefits, meeting consumer demand for nutritious and functional foods.

## Conflicts of Interest

The authors declare that there is no conflict of interest regarding the publication of this paper.

## Acknowledgement

The authors would like to express their appreciation for the financial support provided by the Faculty of Food Science and Nutrition at Universiti Malaysia Sabah. The research was funded in part by Universiti Malaysia Sabah through Skim Pensyarah Lantikan Baru (SLB2234).

## References

- [1] Zhang, N., & Ma, G. (2016). Noodles, traditionally and today. *Journal of Ethnic Foods*, 3(3), 209–212. <https://doi.org/10.1016/j.jef.2016.08.003>
- [2] Fu, B. X. (2008). Asian noodles: History, classification, raw materials, and processing. *Food Research International*, 41(9), 888–902. <https://doi.org/10.1016/j.foodres.2007.11.007>
- [3] Abd Jalil, M. A., Shuid, A. N., & Muhammad, N. (2012). Role of medicinal plants and natural products on osteoporotic fracture healing. *Evidence-Based Complementary and Alternative Medicine*, 2012, 714512. <https://doi.org/10.1155/2012/714512>
- [4] Lee, J. H., Cho, S., Paik, H. D., Choi, C. W., Nam, K. T., Hwang, S. G., & Kim, S. K. (2014). Investigation on antibacterial and antioxidant activities, phenolic and flavonoid contents of some Thai edible plants as an alternative for antibiotics. *Asian-Australasian Journal of Animal Sciences*, 27(10), 1461–1468. <https://doi.org/10.5713/ajas.2013.13629>
- [5] Hussain, K., Ismail, Z., Sadikun, A., & Ibrahim, P. (2009). Antioxidant, anti-TB activities, phenolic and amide contents of standardised extracts of *Piper sarmentosum* Roxb. *Natural Product Research*, 23(3), 238–249. <https://doi.org/10.1080/14786410801987597>
- [6] Chanwitheesuk, A., Teerawutgulrag, A., & Rakariyatham, N. (2005). Screening of antioxidant activity and antioxidant compounds of some edible plants of Thailand. *Food Chemistry*, 92(3), 491–497. <https://doi.org/10.1016/j.foodchem.2004.07.035>
- [7] Nouri, L., Nafchi, A. M., & Karim, A. A. (2015). Mechanical and sensory evaluation of noodles incorporated with betel leaf extract. *International Journal of Food Engineering*, 11(2), 221–227. <https://doi.org/10.1515/ijfe-2014-0183>
- [8] Utama-ang, N., Cheewinworasak, T., Simawonthamgul, N., & Samakradhamrongthai, R. S. (2020). Influence of garlic and pepper powder on physicochemical and sensory qualities of flavoured rice noodle. *Scientific Reports*, 10(1), 8538. <https://doi.org/10.1038/s41598-020-65198-4>
- [9] Benjamin, M. A. Z., Ng, S. Y., Saikim, F. H., & Rusdi, N. A. (2022). The effects of drying techniques on phytochemical contents and biological activities on selected bamboo leaves. *Molecules*, 27(19), 6458. <https://doi.org/10.3390/molecules27196458>
- [10] Guiné, R. P. F. (2018). The drying of foods and its effect on the physical-chemical, sensorial and nutritional properties. *International Journal of Food Engineering*, 4(2), 93–100. <https://doi.org/10.18178/ijfe.4.2.93-100>
- [11] Syah, H., Tambunan, A. H., Hartulistiyoso, E., & Manalu, L. P. (2020). Kinetika pengeringan lapisan tipis daun jati belanda. *Jurnal Keteknik Pertanian*, 8(2), 53–62. <https://doi.org/10.19028/jtep.08.2.53-62>
- [12] Bonazzi, C., & Dumoulin, E. (2011). Quality changes in food materials as influenced by drying processes. In E. Tsotsas & A. S. Mujumdar (Eds.), *Modern Drying Technology* (Vol. 3, pp. 1–20). Hoboken, NJ, USA: Wiley-VCH. <https://doi.org/10.1002/9783527631667.ch1>
- [13] Vega-Gálvez, A., Di Scala, K., Rodríguez, K., Lemus-Mondaca, R., Miranda, M., López, J., & Perez-Won, M. (2009). Effect of air-drying temperature on physico-chemical properties, antioxidant capacity, colour and total phenolic content of red pepper (*Capsicum annuum*, L. var. Hungarian). *Food Chemistry*, 117(4), 647–653. <https://doi.org/10.1016/j.foodchem.2009.04.066>



- [14] Alfeo, V., Planeta, D., Velloso, S., Palmeri, R., & Todaro, A. (2021). Cherry tomato drying: Sun versus convective oven. *Horticulturae*, 7(3), 40. <https://doi.org/10.3390/horticulturae7030040>
- [15] Chibuzo, N. S., Osinachi, U. F., James, M. T., Chigozie, O. F., Dereje, B., & Irene, C. E. (2021). Technological advancements in the drying of fruits and vegetables: A review. *African Journal of Food Science*, 15(12), 367–379. <https://doi.org/10.5897/AJFS2021.2113>
- [16] Pratama, Y., Abduh, S. B. M., Legowo, A. M., Pramono, Y. B., & Albaarri, A. N. (2018). Optimum carrageenan concentration improved the physical properties of cabinet-dried yoghurt powder. *IOP Conference Series: Earth and Environmental Science*, 102(1), 012023. <https://doi.org/10.1088/1755-1315/102/1/012023>
- [17] Li, M., Ma, M., Zhu, K.-X., Guo, X.-N., & Zhou, H.-M. (2017). Delineating the physico-chemical, structural, and water characteristic changes during the deterioration of fresh noodles: Understanding the deterioration mechanisms of fresh noodles. *Food Chemistry*, 216, 374–381. <https://doi.org/10.1016/j.foodchem.2016.08.059>
- [18] Stephenus, F. N., Benjamin, M. A. Z., Anuar, A., & Awang, M. A. (2023). Effect of temperatures on drying kinetics, extraction yield, phenolics, flavonoids, and antioxidant activity of *Phaleria macrocarpa* (Scheff.) Boerl. (mahkota dewa) fruits. *Foods*, 12(15), 2859. <https://doi.org/10.3390/foods12152859>
- [19] Lewis, W. K. (1921). The rate of drying of solid materials. *The Journal of Industrial and Engineering Chemistry*, 13(5), 427–432. <https://doi.org/10.1093/nq/175.27.477-a>
- [20] Page, G. E. (1949). Factors influencing the maximum rates of air drying shelled corn in thin layers [Purdue University, West Lafayette, IN, USA]. Retrieved from <http://dx.doi.org/10.1016/j.jaci.2012.05.050>
- [21] Henderson, S. M., & Pabis, S. (1961). Grain drying theory. I. Temperature effect on drying coefficients. *Journal of Agricultural Engineering Research*, 6, 169–174.
- [22] Sharaf-Eldeen, Y., Blaisdell, J., & Hamdy, M. (1980). A model for ear corn drying. *Transactions of the ASAE*, 23(5), 1261–1265. <https://doi.org/10.13031/2013.34757>
- [23] Midilli, A., & Kucuk, H. (2003). Mathematical modeling of thin layer drying of pistachio by using solar energy. *Energy Conversion and Management*, 44(7), 1111–1122. [https://doi.org/10.1016/S0196-8904\(02\)00099-7](https://doi.org/10.1016/S0196-8904(02)00099-7)
- [24] Fakhruddin, I. M., Ramaiya, S. D., Muta Harah, Z., Nur Leena Wong, W. S., Awang, M. A., & Ismail, N. I. M. (2022). Effects of temperature on drying kinetics and biochemical composition of *Caulerpa lentillifera*. *Food Research*, 6(5), 168–173. [https://doi.org/10.26656/fr.2017.6\(5\).637](https://doi.org/10.26656/fr.2017.6(5).637)
- [25] Chandra, P. K., & Singh, R. P. (1994). *Applied Numerical Methods for Food and Agricultural Engineers* (1st ed.). CRC Press.
- [26] Awang, M. A., Chua, L. S., Abdullah, L. C., & Pin, K. Y. (2021). Drying kinetics and optimization of quercetin extraction from *Melastoma malabathricum* leaves. *Chemical Engineering and Technology*, 44(7), 1214–1220. <https://doi.org/10.1002/ceat.202100007>
- [27] Erbay, Z., & Icier, F. (2010). A review of thin layer drying of foods: Theory, modeling, and experimental results. *Critical Reviews in Food Science and Nutrition*, 50(5), 441–464. <https://doi.org/10.1080/10408390802437063>
- [28] Assefa, A. D., Choi, S., Lee, J. E., Sung, J. S., Hur, O. S., Ro, N. Y., Lee, H. S., Jang, S. W., & Rhee, J. H. (2019). Identification and quantification of selected metabolites in differently pigmented leaves of lettuce (*Lactuca sativa* L.) cultivars harvested at mature and bolting stages. *BMC Chemistry*, 13(3), 56. <https://doi.org/10.1186/s13065-019-0570-2>
- [29] Jinoni, D. A., Benjamin, M. A. Z., Mus, A. A., Goh, L. P. W., Rusdi, N. A., & Awang, M. A. (2024). *Phaleria macrocarpa* (Scheff.) Boerl. (mahkota dewa) seed essential oils: Extraction yield, volatile components, antibacterial, and antioxidant activities based on different solvents using Soxhlet extraction. *Kuwait Journal of Science*, 51, 100173. <https://doi.org/10.1016/j.kjs.2023.100173>
- [30] Awang, M. A., Benjamin, M. A. Z., Anuar, A., Ismail, M. F., Ramaiya, S. D., & Mohd Hashim, S. N. A. (2023). Dataset of gallic acid quantification and their antioxidant and anti-inflammatory activities of different solvent extractions from *kacip fatimah* (*Labisia pumila* Benth. & Hook. f.) leaves. *Data in Brief*, 51, 109644. <https://doi.org/10.1016/j.dib.2023.109644>
- [31] Ndukwu, M. C., Ibeh, M., Ekop, I., Abada, U., Etim, P., Bennamoun, L., Abam, F., Simo-Tagne, M., & Gupta, A. (2022). Analysis of the heat transfer coefficient, thermal effusivity and mathematical modelling of drying kinetics of a partitioned single pass low-cost solar drying of cocoyam chips with economic assessments. *Energies*, 15(12), 4457. <https://doi.org/10.3390/en15124457>
- [32] Bassey, E. J., Cheng, J.-H., & Sun, D.-W. (2022). Thermoultrasound and microwave-assisted freeze-thaw pretreatments for improving infrared drying and quality characteristics of red dragon fruit slices. *Ultrasonics Sonochemistry*, 91, 106225. <https://doi.org/10.1016/j.ultsonch.2022.106225>
- [33] Vega-Gálvez, A., Uribe, E., Gómez-Pérez, L. S., García, V., Mejías, N., & Pastén, A. (2022). Drying kinetic modeling and assessment of mineral content, antimicrobial activity, and potential  $\alpha$ -glucosidase activity inhibition of a green seaweed (*Ulva spp.*) subjected to different drying methods. *ACS Omega*, 7(38), 34230–34238. <https://doi.org/10.1021/acsomega.2c03617>
- [34] Gasa, S., Sibanda, S., Workneh, T. S., Laing, M., & Kassim, A. (2022). Thin-layer modelling of sweet potato slices drying under naturally-ventilated warm air by solar-venturi dryer. *Heliyon*, 8(2), e08949. <https://doi.org/10.1016/j.heliyon.2022.e08949>
- [35] Yao, C., Qian, X.-D., Zhou, G.-F., Zhang, S.-W., Li, L.-Q., & Guo, Q.-S. (2019). A comprehensive analysis and comparison between vacuum and electric oven drying methods on Chinese saffron (*Crocus sativus* L.). *Food Science and Biotechnology*, 28(2), 355–364. <https://doi.org/10.1007/s10068-018-0487-x>
- [36] Onwude, D. I., Hashim, N., Janius, R. B., Nawi, N. M., & Abdan, K. (2016). Modeling the thin-layer drying of fruits and vegetables: A review. *Comprehensive Reviews in Food Science and Food Safety*, 15(3), 599–618. <https://doi.org/10.1111/1541-4337.12196>
- [37] Kucuk, H., Midilli, A., Kilic, A., & Dincer, I. (2014). A review on thin-layer drying-curve equations. *Drying Technology*, 32(7), 757–773. <https://doi.org/10.1080/07373937.2013.873047>
- [38] Chasiotis, V., Tzempelikos, D., & Filios, A. (2021). Evaluation of a moisture diffusion model for analyzing the convective drying kinetics of *Lavandula x allardii* leaves. *Computation*, 9(12), 141.



- <https://doi.org/10.3390/computation9120141>
- [39] Rocha, R. P., Melo, E. C., & Radünz, L. L. (2011). Influence of drying process on the quality of medicinal plants: A review. *Journal of Medicinal Plant Research*, 5(33), 7076–7084. <https://doi.org/10.5897/JMPRx11.001>
- [40] Nguyen, T. V. L., Nguyen, M. D., Nguyen, D. C., Bach, L. G., & Lam, T. D. (2019). Model for thin layer drying of lemongrass (*Cymbopogon citratus*) by hot air. *Processes*, 7(1), 21. <https://doi.org/10.3390/pr7010021>
- [41] Doymaz, I. (2010). Evaluation of mathematical models for prediction of thin-layer drying of banana slices. *International Journal of Food Properties*, 13(3), 486–497. <https://doi.org/10.1080/10942910802650424>
- [42] Sacilik, K. (2007). Effect of drying methods on thin-layer drying characteristics of hull-less seed pumpkin (*Cucurbita pepo* L.). *Journal of Food Engineering*, 79(1), 23–30. <https://doi.org/10.1016/j.jfoodeng.2006.01.023>
- [43] Rababah, T. M., Al-u'datt, M., Alhamad, M., Al-Mahasneh, M., Ereifej, K., Andrade, J., Altarifi, B., Almajwal, A., & Yang, W. (2015). Effects of drying process on total phenolics, antioxidant activity and flavonoid contents of common Mediterranean herbs. *International Journal of Agricultural and Biological Engineering*, 8(2), 145–150. <https://doi.org/10.3965/j.ijabe.20150802.1496>
- [44] Al-Hamdani, A., Jayasuriya, H., Pathare, P. B., & Al-Attabi, Z. (2022). Drying characteristics and quality analysis of medicinal herbs dried by an indirect solar dryer. *Foods*, 11(24), 4103. <https://doi.org/10.3390/foods11244103>
- [45] Babu, A. K., Kumaresan, G., Raj, V. A. A., & Velraj, R. (2018). Review of leaf drying: Mechanism and influencing parameters, drying methods, nutrient preservation, and mathematical models. *Renewable and Sustainable Energy Reviews*, 90, 536–556. <https://doi.org/10.1016/j.rser.2018.04.002>
- [46] Ifrada, R. A. R., Martati, E., & Estiasih, T. (2022). Extraction optimization propolis in the functional drink of keprok batu 55 orange (*Citrus reticulata* Blanco). *Jurnal Pangan Dan Agroindustri*, 10(4), 224–234. <https://doi.org/10.21776/ub.jpa.2022.010.04.5>
- [47] Wang, L., Yang, B., Du, X., & Yi, C. (2008). Optimisation of supercritical fluid extraction of flavonoids from *Pueraria lobata*. *Food Chemistry*, 108(2), 737–741. <https://doi.org/10.1016/j.foodchem.2007.11.031>
- [48] Ngamsuk, S., Huang, T.-C., & Hsu, J.-L. (2020). Determination of phenolic compounds, procyanidins, and antioxidant activity in processed *Coffea arabica* L. leaves. *Foods*, 8(9), 389. <https://doi.org/10.3390/foods8090389>
- [49] Sadek, N. F., & Hamidah, R. S. (2023). The stability of total phenolic and antioxidant activity during processing and cooking of sorghum-moringa substituted tapioca noodle. *IOP Conference Series: Earth and Environmental Science*, 1169(1), 012096. <https://doi.org/10.1088/1755-1315/1169/1/012096>
- [50] Ahmad, Z., Ilyas, M., Ameer, K., Khan, M. A., Waseem, M., Shah, F.-H., Mehmood, T., Rehman, M. A., & Mohamed Ahmed, I. A. (2022). The influence of fenugreek seed powder addition on the nutritional, antioxidant, and sensorial properties of value-added noodles. *Journal of Food Quality*, 2022, 4940343. <https://doi.org/10.1155/2022/4940343>
- [51] Aryal, S., Baniya, M. K., Danekhu, K., Kunwar, P., Gurung, R., & Koirala, N. (2019). Total phenolic content, flavonoid content and antioxidant potential of wild vegetables from western Nepal. *Plants*, 8(4), 96. <https://doi.org/10.3390/plants8040096>
- [52] Lu, Y., & Foo, L. Y. (2001). Antioxidant activities of polyphenols from sage (*Salvia officinalis*). *Food Chemistry*, 75(2), 197–202